

# Numerical Simulation of Transverse Jet Interaction with Rudders in Supersonic Free Stream for Simplified Missile

*Li Longfei, Wang Jiangfeng\**

College of Aerospace Engineering, Nanjing University of Aeronautics and Astronautics, Nanjing 210016, P. R. China

(Received 10 March 2018; revised 20 March 2018; accepted 20 May 2018)

**Abstract:** Numerical simulation is carried out for jets arranged at 7 different positions for the same model and compared with non-jet flows. The total and rudder force and moment amplification is calculated and analyzed by the pressure distribution on the surface and rudders of the simplified missile. Numerical results show that interactions take great effect on the configuration of the flow field around rudders and the pressure distribution on the missile surface.

**Key words:** amplification factor; transverse jet interaction; numerical analysis; rudder

**CLC number:** V21      **Document code:** A      **Article ID:** 1005-1120(2018)S-0016-04

## 0 Introduction

Rapider maneuverability and quicker response time are usually the requirement of supersonic air-to-air missiles to hit the target accurately. Reaction control system (RCS) has several advantages over traditional aerodynamic control surface, especially when operating in low dynamic pressure (low velocity or high altitude)<sup>[1]</sup>. Former researches show that reaction control on air-vehicles results in an interaction flow field between oncoming main stream and jet plume which results in an external aerodynamic jet-interaction force and moment<sup>[2]</sup>. Both positive and negative effect can be obtained when jet location and jet flow characteristics are different.

A number of experimental and numerical studies has been carried out for RCS. Dennis computationally and experimentally performed a sonic injection into a Mach 3.0 free stream<sup>[3]</sup>. Aswin systematically studied the interference effects of side jets with supersonic cross flow for a transverse jet controlled missile, the effect of angle of attack, ratios of free stream and jet pressure are analyzed<sup>[4]</sup>. Graham numerically investi-

gated the interaction between a lateral jet and the external flow for several axisymmetric bodies. The mass flow and flight velocity have the most significant effect on the force and moments<sup>[5]</sup>.

In a great deal of researches on RCS, the interaction between jet and rudders is rarely considered and studied. In this work, the interaction between transverse cold jet which contains 7 jet nozzles on the simplified missile located in series uniformly in front of or between X-shape rudders ejected from the missile body and rudders in Mach 4.5 oncoming free stream and altitude 10 km is numerically studied. The flow fields with different jet locations are predicted and compared with non-jet flow. Global and rudder force and moment amplification factors of the missile are calculated and analyzed by the pressure distribution on rudders beside jet nozzles and missile body when 7 jets work respectively.

## 1 Geometry and Computational Methodology

### 1.1 Geometry Description

To study the interaction between jet flow,

\*Corresponding author, E-mail address: wangjf@nuaa.edu.cn.

free stream and rudders, the missile model is simplified to a combination of a slender, a pair of X-shape rudders and 7 jet nozzles, as shown in Fig. 1. The nose part (length  $3.5 D$ ) is made up of a Carman curve profile cross section, where  $D$  is the diameter of the slender. 7 circular, sonic transverse-jet nozzles of  $20\text{mm}$  ( $0.1 D$ ) in diameter are located on the cylinder (length  $15.75 D$ ), the 1<sup>st</sup> jet nozzle is located at  $3.55 D$  downstream from the nose and the other jet nozzles are located  $0.25 D$  downstream from each previous one. The root of leading edge of the trapezoid X-shape rudders are located  $4 D$  downstream from the nose.

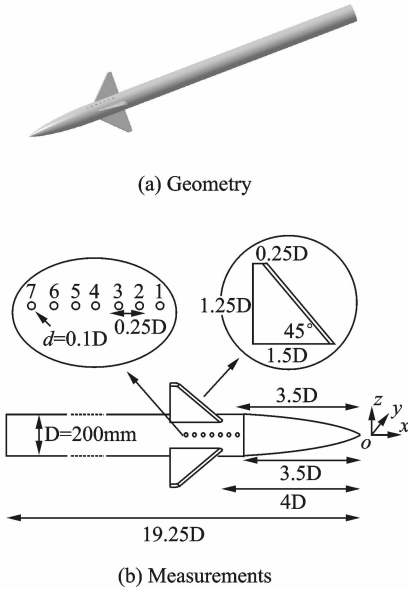


Fig. 1 Geometry and measurements

Structured grid is generated and the missile mesh on the surface is shown in Fig. 2. More grids are distributed around jet nozzles. After verifying independence of the mesh distribution,  $71 \times 240 \times 208$  is fine enough to be selected.

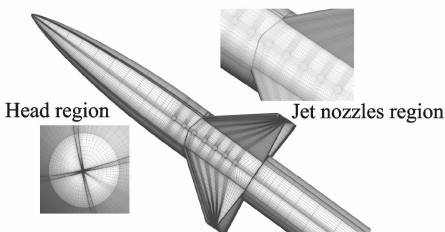


Fig. 2 Computational mesh

## 1.2 Computational Methodology

Three-dimensional reynolds-average Navier-

Stokes (RANS) equations based on finite volume approach along with Spalart-Allmaras (S-A) turbulence model on structured grid are solved. Temporal discretization and spatial discretization are carried out with the lower-upper symmetric Gauss-Seidel (LU-SGS) method and second-order Roe scheme respectively.

The magnitudes of the jet force and moment and the jet-interaction force and moment can be compared through jet-interaction amplification factors  $K_F$  and  $K_M$ , as shown in Eq. (1) and (2). An amplification factor greater than 1 means the jet-interaction force and moment amplifies or increases the total ones produced by the jet, whereas an amplification factor less than 1 indicates that the jet-interaction force and moment reduces the total ones after interaction.

$$K_F = 1 + \frac{F_{\text{jeton}} - F_{\text{jetoff}}}{F_j} \quad (1)$$

$$K_M = 1 + \frac{M_{\text{jeton}} - M_{\text{jetoff}}}{M_j} \quad (2)$$

$$F_j = (\rho_j V_j^2 + p_{sj} - p_\infty) S_j \quad (3)$$

$$M_j = F_j L_j \quad (4)$$

$F_{\text{jeton}}$  and  $M_{\text{jeton}}$  indicate the force and moment when jets work. The subscript jetoff indicates the force and moment when jets off.  $F_j$  and  $M_j$  are the jet ejection force and moment.  $\rho_j$  is the density of jet flow,  $V_j$  is the ejection velocity,  $p_{sj}$  is the static pressure of jet media,  $p_\infty$  is the free stream static pressure and the  $S_j$  means the outlet area of every single jet.

$K_{Fr}$  and  $K_{Mr}$  are the force and moment amplification caused by rudders as shown in Eq. (5) and Eq. (6)

$$K_{Fr} = \frac{F_r}{F_j} \quad (5)$$

$$K_{Mr} = \frac{M_r}{M_j} \quad (6)$$

where  $F_r$  and  $M_r$  are the force and moment on rudders. Non-dimensional pressure is shown in Eq. (7)

$$p = \frac{\tilde{p}}{\tilde{\rho}_\infty (\tilde{a}_\infty)} \quad (7)$$

where  $\tilde{\rho}_\infty$  is the dimensional free-stream density, and the  $\tilde{a}_\infty$  is the dimensional free-stream speed of sound.

## 2 Results and Discussion

The computational conditions of free stream are shown in Table 1 and the computational conditions of jet flow are shown in Table 2. The free stream conditions of both cases are the same. Case 1 is the non-jet flow and Case 2 is the flow with specific jet conditions.

**Table 1 Free stream conditions**

Case	$Ma_\infty^a$	$p_\infty/\text{MPa}^b$	$T_\infty/\text{K}^c$
1	4.5	0.266	223.3
2	4.5	0.266	223.3

Superscript “a” the Mach number of free stream. Superscript “b” the static pressure of free stream. Superscript “c” the static temperature of free stream.

**Table 2 Jet flow conditions**

Case	Jet	$Ma_j^a$	$p_j/\text{MPa}^b$	$T_j/\text{K}^c$	$R_p^d$
1					
2	1 <sup>#</sup> —7 <sup>#</sup>	1.0	45.316	267.9	90

Superscript “a” represent the Mach number of jet flow. Superscript “b” the total pressure of jet flow. Superscript “c” the Total temperature of jet flow. Superscript “d” the static pressure ratio of jet flow and free stream.

The specific heat ratio  $\lambda$  of both jet flow and free stream is constant to 1.4.

Global force and moment amplifications of jet flows when jet works from 1<sup>#</sup> to 7<sup>#</sup> respectively are shown in Table 3.

**Table 3 Jet flow conditions**

Parameter	1 <sup>#</sup>	2 <sup>#</sup>	3 <sup>#</sup>	4 <sup>#</sup>	5 <sup>#</sup>	6 <sup>#</sup>	7 <sup>#</sup>
Force	2.60	2.83	1.36	1.23	1.10	0.97	0.90
Moment	2.79	3.08	1.49	1.41	1.32	1.24	1.20

For all cases simulated, the 2<sup>#</sup> jet meets the maximum force and moment amplification factor. The force and moment amplification decreases when the location of the jet moves away from the slender nose. Fig. 3 presents the non-dimensional pressure distributions on rudders. The right half indicates the jet side rudder, and the left half illustrated the pressure distributions on the reverse side. The figures of 2<sup>#</sup> jet have the largest area of high pressure region on jet side of the rudder with

same contour range. On the jet side rudder surface, from 3<sup>#</sup> to 7<sup>#</sup> jet, the area of high pressure region decreases but bigger than the non-jet flow and located closer to the root of trailing edge of the rudder. Comparing with the reverse side rudder surface of jet flows, the pressure on jet side are always greater than the reverse side which provides positive lift that makes force and moment amplification factors greater than 1.

The total force, moment amplification factors, the rudder force and moment amplification factors are shown in Fig. 4. The rudder force and moment amplification factors are always greater than total ones, which means the force and moment of the slender are mostly contributed by the interaction between jet flow and rudders in the oncoming free stream. When the location of the jet nozzle moves downstream from 2<sup>#</sup> jet, the interaction area on the rudders decreases which causes a decrease of rudder and total force amplification factors.

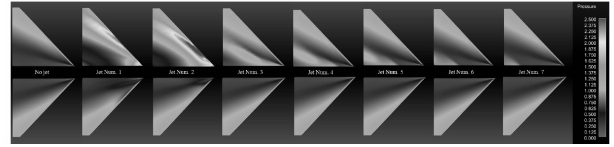


Fig. 3 Pressure distribution on rudders

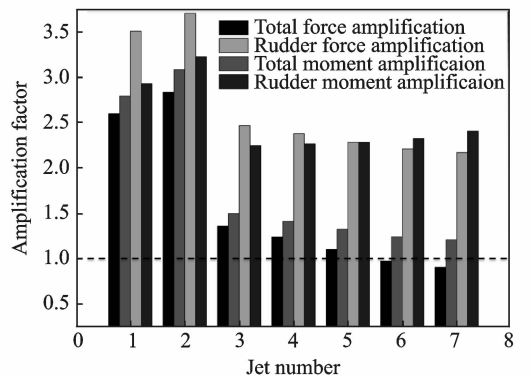


Fig. 4 Force and moment amplification factors

Cutting the model by  $x-z$  plane into upper half ( $y > 0$ ) and lower half ( $y < 0$ ) with jet nozzles. The pressure coefficient distributions on sections normal to  $x$  axis are shown in Fig. 5 to Fig. 7. The pressure coefficients on upper half are always greater than those on lower half where negative lift is produced that makes the total force

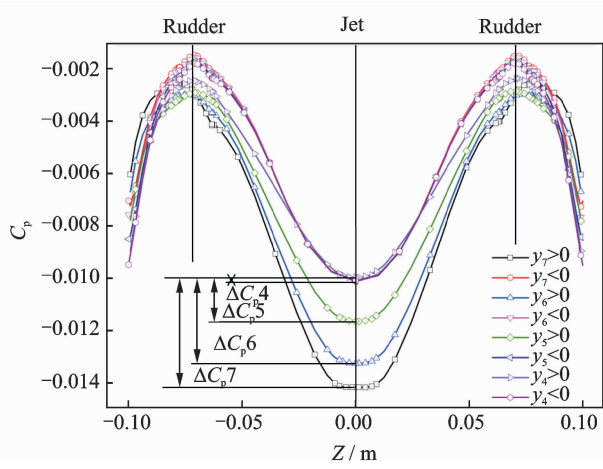


Fig. 5  $C_p$  distribution on slender body at  $X=1.5$  m

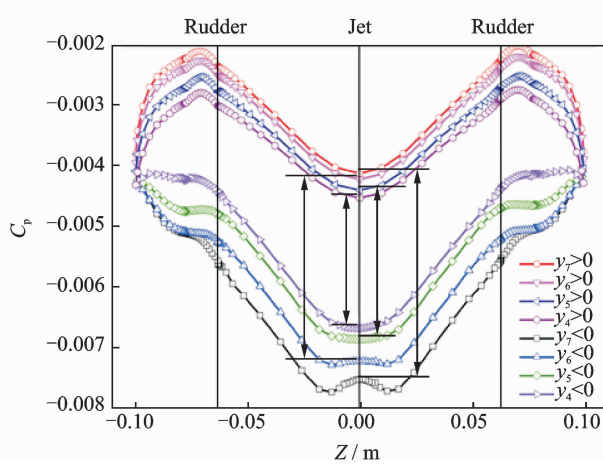


Fig. 6  $C_p$  distribution on slender body at  $X=1.75$  m

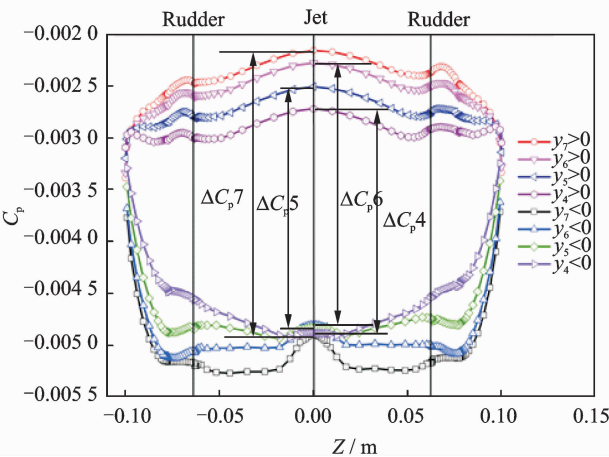


Fig. 7  $C_p$  distribution on slender body at  $X=2.0$  m

amplification factor of 6<sup>#</sup> and 7<sup>#</sup> jet less than 1.

### 3 Conclusions

In this work, one non-jet case and three jet cases with different jet flow conditions of a slender body in the oncoming free stream at Mach 4.5

is simulated. Comparing the jet cases with the non-jet case, the interaction of jet flow and rudders takes great effect on the force and moment of the slender body. The pressure which is different on the jet side and reverse side will results in force and moment amplification. For the three jet cases, the jet flow ejected from 2<sup>#</sup> jet nozzle has the strongest interaction with the X-shape rudders and reaches the greatest force and moment amplification factors.

### Acknowledgement

This work was supported in part by Fundamental of Graduate Innovation Center in NUAU (No. kfj20170122) and the Fundamental Research Funds for the Central Universities.

### References:

- [1] DESPIRITO J. Factors affecting reaction jet interaction effect on projectiles[C]// AIAA Applied Aerodynamics Conference. [S. l.]:AIAA,2011:1-22.
- [2] CASSEL L A. Applying jet interaction technology [J]. J Spacecraft & Rockets,2003,40(4): 523-537.
- [3] ZHAO F M, WANG J F. Analysis on flow field characteristics of lateral jet on slender body[J], J Aerosp Power, 2016,31(3): 726-732.
- [4] VITI V, SCHETZ J A. Numerical studies of the jet interaction flowfield with main jet and an array of smaller jets[C]// ICAS. [S. l.]:[s. n.],2002:1-11.
- [5] ASWIN G, CHAKRABORTY D. Numerical simulation of transverse side jet interaction with supersonic free stream[J]. Aerosp Sci Technol, 2010,14(5): 295-301.

Mr. **Li Longfei** is a Ph. D candidate in Nanjing University of Aeronautics and Astronautics, Nanjing, China. His research interest focuses on numerical high-speed aerodynamics and applications.

Prof. **Wang Jiangfeng** received his Ph. D degree in fluid mechanics from Nanjing University of Aeronautics and Astronautics in 2000. He is currently a professor of college of aerospace engineering in Nanjing University of Aeronautics and Astronautics. His research interests include the combustion flow field simulation, high-speed chemical nonequilibrium flow field simulation, etc.